



Cite this: *Chem. Commun.*, 2025, 61, 10855

Received 28th February 2025,  
Accepted 2nd June 2025

DOI: 10.1039/d5cc01101a

rsc.li/chemcomm

# Utilizing enantiomerically pure organic spacers for anion-centred clusters in a hybrid inorganic–organic lead-halide crystal†

Markus W. Heindl,<sup>a</sup> Joachim Ballmann<sup>b\*</sup> and Felix Deschler<sup>\*a</sup>

**In this work, we present structural data of the novel, chiral material (S-2AH)<sub>4</sub>[Pb<sub>2</sub>Br<sub>7</sub>]Br obtained from single crystal X-ray diffraction (SCXRD). This quasi-2D material displays anion-centred clusters within its organic layer, without the need for bi-functional spacers. Instead, the structure is based on the steric properties of the used enantiomerically pure precursors.**

Over recent years chiral lead-halide perovskites have evolved from a structural curiosity into a key point of interest for material science.<sup>1</sup> They can be fabricated through relatively simple, solution-based strategies while also displaying sought-after optoelectronic properties. These include the preferred absorption and emission of one form of circularly polarized light as well as creating spin-polarized electrical currents *via* the chirality-induced spin selectivity (CISS) effect.<sup>1–6</sup> Particularly their use for the transfer of spin-polarized charge carriers has become a focus point of research over the past few years.<sup>7–9</sup> Recent studies have suggested that these phenomena originate from slight structural distortions that occur when enantiomerically pure organic spacers are used instead of a racemic mixture.<sup>10–12</sup> However, as a less discussed aspect, these alterations can also be much more pronounced.<sup>13</sup> This opens an opportunity for the design of novel materials by utilizing the specific steric properties of pure enantiomers compared to their racemic mixtures. In this work, we will demonstrate the use of (*S*)-2-aminoheptane (*S*-2AH) to form a novel 2D-structure that allows for the incorporation of anion-centred clusters within the organic layer.

For this we add 0.18 g of PbBr<sub>2</sub> (0.49 mmol, Sigma-Aldrich, ≥98%) into 2 mL of concentrated hydrobromic acid (Sigma-Aldrich, 48%) and cool the mixture in an ice-bath before adding

dropwise 0.1466 mL of (*S*)-2-aminoheptane (0.97 mmol, Sigma-Aldrich, 99%). The resulting mixture is then placed in an autoclave and heated to 90 °C. After 12 h it is then cooled back to room temperature at a rate of −1 °C h<sup>−1</sup>. The result are clear, needle-shaped crystals at a yield of 14%.

Analysis with SCXRD reveals a layered structure composed of inorganic lead-bromide sheets separated by organic spacers (see Fig. 1). This material's unit cell has the elemental composition C<sub>112</sub>H<sub>288</sub>Br<sub>32</sub>N<sub>16</sub>Pb<sub>8</sub> but is perhaps better described as (S-2AH)<sub>4</sub>[Pb<sub>2</sub>Br<sub>7</sub>]Br due to its composition out of units of two face-sharing octahedra and the isolated bromide anion within the organic layer. Further, due to the low-density packing of the spacer molecules, some carbon atoms of the heptyl chain were found to be disordered without affecting the stereogenic centre at the 2-position (see Fig. S1, ESI†). The material crystallizes in the polar non-centrosymmetric Sohncke space group *P*<sub>2</sub><sub>1</sub><sub>2</sub><sub>1</sub><sub>2</sub><sub>1</sub> and is therefore chiral (Flack *x*: −0.048(16), Hooft *y*: −0.034(4), Parson's *q*: −0.056(5), Bijvoet pairs coverage: 0.98 with *P*<sub>2</sub>(true) = 1.000, see ESI† for details).<sup>1</sup> Purity is confirmed by combustion analysis (see Table S2, ESI†).

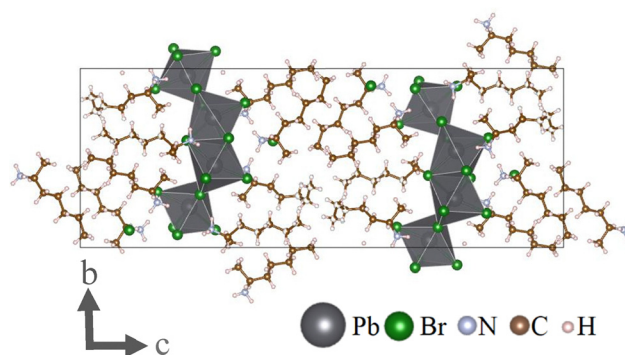


**Fig. 1** The unit cell of (S-2AH)<sub>4</sub>[Pb<sub>2</sub>Br<sub>7</sub>]Br consist of two inorganic layers made up of lead-bromide octahedra. These layers are separated by organic spacers in which a bromide anion is located. Disordered atoms omitted for clarity. This graphic was created using the VESTA software package.<sup>14</sup>

<sup>a</sup> Physikalisch-Chemisches Institut, Universität Heidelberg, Im Neuenheimer Feld 229, D-69120 Heidelberg, Germany. E-mail: [deschler@uni-heidelberg.de](mailto:deschler@uni-heidelberg.de)

<sup>b</sup> Anorganisch-Chemisches Institut, Universität Heidelberg, Im Neuenheimer Feld 276, D-69120 Heidelberg, Germany. E-mail: [na150@uni-heidelberg.de](mailto:na150@uni-heidelberg.de)

† Electronic supplementary information (ESI) available. See DOI: <https://doi.org/10.1039/d5cc01101a>



While the crystal's inorganic layers consist of lead-bromide octahedra, these are not arranged in one of the more established patterns, two of the best known of which perhaps are 2D networks of corner-linked octahedra (commonly known as 2D perovskites) and 1D chains of face-linked octahedra.<sup>13,15</sup> Instead, the inorganic layers alternate between these two structural motives. The result are units of two face-linked octahedra that are each bound to four similar pairs to form a net-like structure (see Fig. 2a). This system is stabilized by the cationic  $-\text{NH}_3^+$  moiety of one organic spacer that is located in the centre of each hole. It is also worth mentioning that – unlike a classic quasi-2D perovskite – the inorganic layers are not planar. Instead, each face-sharing octahedra pair is alternately sticking out above or below a virtual plane as seen in Fig. 2b. We have hence chosen to refer to this two-dimensional net-like structure as “quasi-2D”, to account for this apparent roughness. From this representation it is also apparent that there is another bromide ion that is not part of any octahedron, nor directly linked to the inorganic layer. Instead, this anion is located inside the nonpolar organic spacer region.

Looking at this odd bromide ion, we find that it is surrounded by four positive charges in the form of protonated

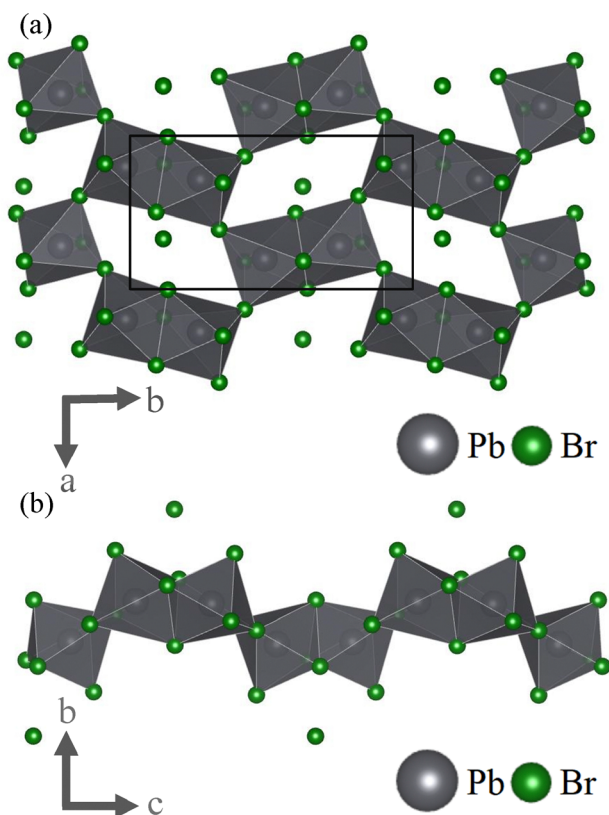


**Fig. 2** Inorganic components of  $(S\text{-}2\text{AH})_4[\text{Pb}_2\text{Br}_7]\text{Br}$  displayed without the organic spacers, as viewed along the (a)  $c$ - and the (b)  $a$ -axis. The inorganic layer is composed out of units of two face-sharing octahedra which in turn are connected through shared corners, forming a net-like structure. Additional bromide-ions are located above or below the resulting holes of the inorganic network. Black lines in figure (a) indicate an exemplary unit cell. This graphic was created using the VESTA software package.<sup>14</sup>

amino groups  $-\text{NH}_3^+$  of the organic spacer cations located between this anion and the inorganic layer. However, this bromide can only form hydrogen bonds with three of these protonated amino groups at the respective distances of 2.39653(4) Å, 2.45616(7) Å and 2.46708(4) Å, resulting in a distorted trigonal pyramid. The fourth protonated amino group is facing in the opposite direction, while the respective molecule's nonpolar tail is placed between the two, resulting in a much greater distance of over 5 Å, too large to be considered a potential hydrogen-bond. This protonated amino group hence binds to the neighbouring interlayer bromide ion. This particular structure can only form since all relevant protonated amino groups are facing towards the same side of their respective alkyl groups (see Fig. 3). This is a strong indication that this is the direct result of the use of enantiomerically pure organic precursors, since otherwise the cationic group would be oriented randomly towards either side of the carbon chain, or the alkyl-group would be forced to take a position that is sterically more demanding. Either option is likely not energetically favourable. Indeed, if the synthesis is repeated with a racemic mixture of 2-Aminoheptane, no single crystals are formed. There are however literature reports that suggest the existence of a classic 2D lead-bromide perovskite utilizing (*rac*)-2-Aminohaptane as spacer, indicating that the structure presented here is likely not formed under the tested fabrication conditions when using racemic precursors.<sup>16</sup> It is further worth noting that – as seen in Fig. 3 – all protonated amino groups binding to the bromide ion are located between the inorganic

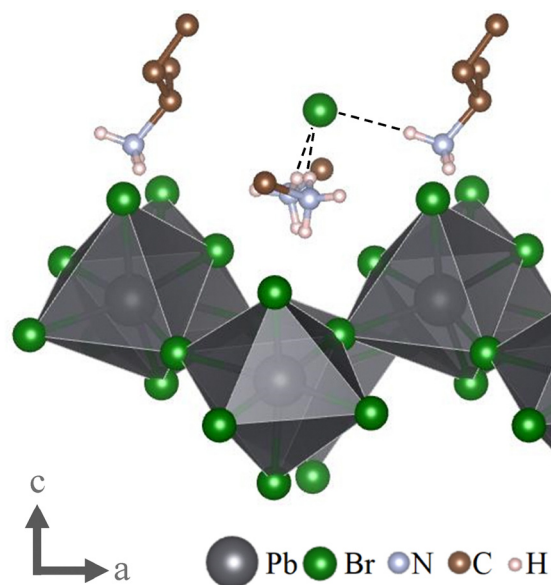


**Fig. 3** The interlayer bromide ion with the four surrounding  $-\text{NH}_3^+$ -moieties. While three of these protonated amino groups form hydrogen bonds with the central anion, the fourth (left) faces away relative to its connected alkyl-group. Further, all protonated amino groups are located between the inorganic layer and the central bromide anion, creating a direct interface between the bromide anion and the organic layer. Dashed lines indicate hydrogen bonds. Parts of the organic spacers were omitted for clarity. This graphic was created using the VESTA software package.<sup>14</sup>



layer and said ion. This means that there is no transition mediated by covalently bound polarized groups between this ion and the nonpolar layer as usually is the case for low-dimensional hybrid materials. Instead, we observe a more direct interface between polar and nonpolar components.

The observation of this bromide ion within the organic layer reminds of recent reports by Aubrey *et al.* and a previous study by Mercier and Riou who each reported the synthesis of single crystals made up of alternating layers of perovskite sheets and other inorganic layers or clusters separated through bi-functional organic spacers, thereby potentially opening up a new strategy for the design of functional materials.<sup>17,18</sup> This approach has already been successfully demonstrated to add antiferromagnetic coupling effects to an otherwise diamagnetic perovskite-like lead-halide material by incorporating transition-metal clusters into the crystal structure.<sup>19</sup> Others have found that this material class can display increased resistance towards air and moisture and have pointed out its anisotropic charge transport properties.<sup>20</sup> However, our material differs in a few key points. First, the structure presented here still possesses a van der Waals gap since the individual layers are not linked through covalent bonds. This may enable quantum confinement effects.<sup>21</sup> Second, while in other structures the non-perovskite layer or cluster usually forms though the direct interaction of the organic spacers or is centred around one or multiple (metal-) cations, here the inorganic heterostructure is centred around a bromide anion, making this – to the best of our knowledge – the first reported anion-centred interlayer cluster. Further, unlike previously reported materials displaying interlayer clusters, (S-2AH)<sub>4</sub>[Pb<sub>2</sub>Br<sub>7</sub>]Br is chiral and could hence be utilized for chiroptic and spintronic applications.<sup>1</sup> Finally, while previous works have relied on bi-functional organic spacers to create these kinds of heterostructures, the material presented here merely relies on the steric properties of mono-functional (S)-2-aminoheptane. We therefore believe that this crystal structure represents an interesting addition to the pool of materials with interlayer clusters.

To summarize, we report the novel, chiral material (S-2AH)<sub>4</sub>[Pb<sub>2</sub>Br<sub>7</sub>]Br that combines structural motives of well-established 1D and 2D organic–inorganic hybrids often studied in regards to their optoelectronic properties. This material displays unusual anion-centred clusters within its organic layers which are not a result of bi-functional spacers but rather originate from the specific steric properties of the enantiomerically pure precursors used. We believe that this material is a promising candidate for an in-depth investigation of its polar-nonpolar interfaces and the resulting structural effects and properties as for instance piezoelectricity. Further, we hope that this report will help to promote the research on the use of enantiomerically pure precursors in organic–inorganic hybrid materials beyond chiroptic properties and give fresh impulses for the investigation of interlayer clusters.

M. W. H. synthesized the material, evaluated and visualized results and drafted the manuscript. J. B. performed and analysed SCXRD measurements. F. D. supervised the project and guided its direction. All authors reviewed the manuscript and contributed their ideas to its final form.

This project has received funding from the European Research Council (ERC Starting Grant agreement no. 852084-TWIST).

## Data availability

All experimental data, and detailed experimental procedures are available in the ESI.† SCXRD data is available under CCDC 2425604.

## Conflicts of interest

There are no conflicts to declare.

## References

- 1 G. Long, R. Sabatini, M. I. Saidaminov, G. Lakhwani, A. Rasmita, X. Liu, E. H. Sargent and W. Gao, Chiral-perovskite optoelectronics, *Nat. Rev. Mater.*, 2020, 5, 423–439.
- 2 H. Lu, J. Wang, C. Xiao, X. Pan, X. Chen, R. Brunecky, J. J. Berry, K. Zhu, M. C. Beard and Z. V. Vardeny, Spin-dependent charge transport through 2D chiral hybrid lead-iodide perovskites, *Sci. Adv.*, 2019, 5, eaay0571.
- 3 C. Chen, L. Gao, W. Gao, C. Ge, X. Du, Z. Li, Y. Yang, G. Niu and J. Tang, Circularly polarized light detection using chiral hybrid perovskite, *Nat. Commun.*, 2019, 10, 1927.
- 4 S. Liu, M. Kepenekian, S. Bodnar, S. Feldmann, M. W. Heindl, N. Fehn, J. Zerhoch, A. Shcherbakov, A. Pöthig, Y. Li, U. W. Paetzold, A. Kartouzian, I. D. Sharp, C. Katan, J. Even and F. Deschler, Bright circularly polarized photoluminescence in chiral layered hybrid lead-halide perovskites, *Sci. Adv.*, 2023, 9, eadh5083.
- 5 J. Ma, C. Fang, C. Chen, L. Jin, J. Wang, S. Wang, J. Tang and D. Li, Chiral 2D Perovskites with a High Degree of Circularly Polarized Photoluminescence, *ACS Nano*, 2019, 13, 3659–3665.
- 6 I. Abdelwahab, D. Kumar, T. Bian, H. Zheng, H. Gao, F. Hu, A. McClelland, K. Leng, W. L. Wilson, J. Yin, H. Yang and K. P. Loh, Two-dimensional chiral perovskites with large spin Hall angle and collinear spin Hall conductivity, *Science*, 2024, 385, 311–317.
- 7 Q. Wang, H. Zhu, Y. Tan, J. Hao, T. Ye, H. Tang, Z. Wang, J. Ma, J. Sun, T. Zhang, F. Zheng, W. Zhang, H. W. Choi, W. C. H. Choy, D. Wu, X. W. Sun and K. Wang, Spin Quantum Dot Light-Emitting Diodes Enabled by 2D Chiral Perovskite with Spin-Dependent Carrier Transport, *Adv. Mater.*, 2024, 36, e2305604.
- 8 J. Yao, Z. Wang, Y. Huang, J. Xue, D. Zhang, J. Chen, X. Chen, S.-C. Dong and H. Lu, Efficient Green Spin Light-Emitting Diodes Enabled by Ultrafast Energy- and Spin-Funneling in Chiral Perovskites, *J. Am. Chem. Soc.*, 2024, 146, 14157–14165.
- 9 S. Liu, J. Zerhoch, M. W. Heindl, C. Zhang, T. Kodalle, K. Sun, A. Shcherbakov, S. Bodnar, M. Miah, M. Gholipour, C. Jandl, A. Pöthig, J. Ballmann, I. D. Sharp, P. Müller-Buschbaum, C. M. Sutter-Fella, U. W. Paetzold and F. Deschler, Orientation-Driven Chirality Funneling in Chiral Low-Dimensional Lead-Halide Perovskite Heterostructures, *J. Am. Chem. Soc.*, 2025, 147, 16681–16693.
- 10 M. K. Jana, R. Song, H. Liu, D. R. Khanal, S. M. Janke, R. Zhao, C. Liu, Z. Valy Vardeny, V. Blum and D. B. Mitzi, Organic-to-inorganic structural chirality transfer in a 2D hybrid perovskite and impact on Rashba-Dresselhaus spin-orbit coupling, *Nat. Commun.*, 2020, 11, 4699.
- 11 M. K. Jana, R. Song, Y. Xie, R. Zhao, P. C. Serce, V. Blum and D. B. Mitzi, Structural descriptor for enhanced spin-splitting in 2D hybrid perovskites, *Nat. Commun.*, 2021, 12, 4982.
- 12 J. Son, S. Ma, Y.-K. Jung, J. Tan, G. Jang, H. Lee, C. U. Lee, J. Lee, S. Moon, W. Jeong, A. Walsh and J. Moon, Unraveling chirality transfer mechanism by structural isomer-derived hydrogen bonding interaction in 2D chiral perovskite, *Nat. Commun.*, 2023, 14, 3124.
- 13 A. Lemmerer and D. G. Billings, Inorganic–Organic Hybrids Incorporating a Chiral Cyclic Ammonium Cation, *S. Afr. J. Chem.*, 2013, 66, 263–272.



- 14 K. Momma and F. Izumi, VESTA 3 for three-dimensional visualization of crystal, volumetric and morphology data, *J. Appl. Crystallogr.*, 2011, **44**, 1272–1276.
- 15 H. Lin, C. Zhou, Y. Tian, T. Siegrist and B. Ma, Low-Dimensional Organometal Halide Perovskites, *ACS Energy Lett.*, 2018, **3**, 54–62.
- 16 T. Li, W. A. Dunlap-Shohl, E. W. Reinheimer, P. Le Magueres and D. B. Mitzi, Melting temperature suppression of layered hybrid lead halide perovskites via organic ammonium cation branching, *Chem. Sci.*, 2019, **10**, 1168–1175.
- 17 M. L. Aubrey, A. Saldivar Valdes, M. R. Filip, B. A. Connor, K. P. Lindquist, J. B. Neaton and H. I. Karunadasa, Directed assembly of layered perovskite heterostructures as single crystals, *Nature*, 2021, **597**, 355–359.
- 18 N. Mercier and A. Riou, An organic–inorganic hybrid perovskite containing copper paddle-wheel clusters linking perovskite layers:  $[\text{Cu}(\text{O}_2\text{C}-(\text{CH}_2)_3-\text{NH}_3)_2]\text{PbBr}_4$ , *Chem. Commun.*, 2004, 844–845.
- 19 L. Zhao, G. Yao, H. Chen, T. Zeng and Z. Yang, Incorporating Copper(I) Clusters into Lead Halide Perovskite through Mediation of Zwitterionic Linkers, *Chem. Mater.*, 2024, **36**, 3277–3284.
- 20 K. Parashar, Z. Zhang, V. Buturlim, J. Jiang, A. Roseborough, M. Nyman, K. Gofryk, R. Pachter and B. Saparov, Structural and Physical Properties of Two Distinct 2D Lead Halides with Intercalated Cu(II), *J. Mater. Chem. C*, 2024, **12**, 9372–9384.
- 21 S. Wang, Z. Chen, G. Zhao and F. Wang, Quantum confinement effect on the electronic and optical properties of two-dimensional halide perovskites, *Comput. Mater. Sci.*, 2023, **230**, 112524.

